Liver lipid metabolism is altered by increased circulating estrogen to androgen ratio in male mouse

Vehmas, A.P.; Adam, M.; Laajala, T.D.; Kastenmüller, G.; Prehn, C.; Rozman, J.; Ohlsson, C.; Fuchs, H.; de Angelis, M.H.; Gailus-Durner, V.; Elo, L.L.; Aittokallio, T.; Adamski, J.; Corthals, G.; Poutanen, M.; Strauss, L.

DOI
10.1016/j.jprot.2015.12.009

Publication date
2016

Document Version
Final published version

Published in
Journal of Proteomics

Journal of Proteomics 133 (2016) 66–75

Contents lists available at ScienceDirect

Journal of Proteomics

journal homepage: www.elsevier.com/locate/jprot

Liver lipid metabolism is altered by increased circulating estrogen to androgen ratio in male mouse

Anni P. Vehmas [a,b], Marion Adam [b,c], Teemu D. Laajala [c,d,e,f], Gabi Kastenmüller [g], Cornelia Prehn [h], Jan Rozman [i,j,k], Claes Ohlsson [l], Helmut Fuchs [i], Martin Hrabě de Angelis [i,j,m], Valérie Gailus-Durner [i], Laura L. Elo [a,d], Tero Aittokallio [d,f], Jerzy Adamski [h,j,m], Garry Corthals [a,n], Matti Poutanen [b,c,o], Leena Strauss [b,c,*]

[a] Turku Centre for Biotechnology, University of Turku and Åbo Akademi University, Turku, Finland
[b] Department of Physiology, Institute of Biomedicine, University of Turku, Turku, Finland
[c] Turku Center for Disease Modeling, University of Turku, Turku, Finland
[d] Department of Mathematics and Statistics, University of Turku, Turku, Finland
[e] Drug Research Doctoral Programme, University of Turku, Finland
[f] Institute for Molecular Medicine Finland (FIMM), University of Helsinki, Finland
[g] Institute of Bioinformatics and Systems Biology, Helmholtz Zentrum München, Neuherberg, Germany
[h] Genome Analysis Center, Institute of Experimental Genetics, Helmholtz Zentrum München, German Research Center for Environmental Health, Neuherberg, Germany
[i] German Mouse Clinic, Institute of Experimental Genetics, Helmholtz Zentrum München, German Research Center for Environmental Health, Neuherberg, Germany
[j] German Center for Diabetes Research (DZD), Neuherberg, Germany
[k] Molecular Nutritional Medicine, Else Kröner-Fresenius Center, Technische Universität München, Freising-Weihenstephan, Germany
[l] Centre for Bone and Arthritis Research, Institute of Medicine, University of Gothenburg, Gothenburg, Sweden
[m] Experimental Genetics, Center of Life and Food Sciences Weihenstephan, Technische Universität München, Neuherberg, Germany
[n] Van 't Hoff Institute for Molecular Sciences, University of Amsterdam, The Netherlands
[o] Institute of Medicine, Sahlgrenska Academy, University of Gothenburg, Sweden

ARTICLE INFO

Article history:
Received 9 July 2015
Received in revised form 26 October 2015
Accepted 5 December 2015
Available online 9 December 2015

Keywords:
Liver
Aromatase
Male mouse
Label free quantitative proteomics
Metabolomics
Phospholipid

ABSTRACT

Estrogens are suggested to lower the risk of developing metabolic syndrome in both sexes. In this study, we investigated how the increased circulating estrogen-to-androgen ratio (E/A) alters liver lipid metabolism in males. The cytochrome P450 aromatase (P450arom) is an enzyme converting androgens to estrogens. Male mice overexpressing human aromatase enzyme (AROM+ mice), and thus have high circulating E/A, were used as a model in this study. Proteomics and gene expression analyses indicated an increase in the peroxisomal β-oxidation in the liver of AROM+ mice as compared with their wild type littermates. Correspondingly, metabolomic analysis revealed a decrease in the amount of phosphatidylcholines with long-chain fatty acids in the plasma. With interest we noted that the expression of Cyp4a12a enzyme, which specifically metabolizes arachidonic acid (AA) to 20-hydroxy AA, was dramatically decreased in the AROM+ liver. As a consequence, increased amounts of phospholipids having AA as a fatty acid tail were detected in the plasma of the AROM+ mice. Overall, these observations demonstrate that high circulating E/A in males is linked to indicators of higher peroxisomal β-oxidation and lower AA metabolism in the liver. Furthermore, the plasma phospholipid profile reflects the changes in the liver lipid metabolism.

1. Introduction

Estrogens play an important role in male physiology and pathophysiology. The final step in the biosynthesis of estrogens from androgens is catalyzed by the cytochrome P450 aromatase (P450arom). Men with a non-functional aromatase enzyme, and consequently undetectable levels of circulating estrogens, are reported to have tall stature with delayed epiphyseal closure, osteoporosis and impaired reproductive functions [1–3]. In addition, they suffer from metabolic disorder-related symptoms such as dyslipidemia, obesity and insulin resistance, and some of the men have been reported to have liver steatosis [4]. Consistent with human studies, liver steatosis connected to increased circulating triglyceride and cholesterol levels have been detected in aromatase deficient mice (ArKO mice). Dyslipidemia in ArKO mice has been explained by increased lipid biosynthesis, decreased fatty acid β-oxidation and glucose intolerance in the liver [5–7]. The liver phenotype has been shown to normalize after estrogen treatment in both aromatase deficient men and ArKO mice [4,5],

We have previously reported that male mice universally expressing human aromatase enzyme (AROM+ mice), and thus having increased

* Corresponding author at: Department of Physiology, Institute of Biomedicine, University of Turku, FI-20014 Turku, Finland.
E-mail address: leesal@utu.fi (L. Strauss).

http://dx.doi.org/10.1016/j.jprot.2015.12.009
1874-3919/

conversion of androgens to estrogens, are feminized. Although female mice have no phenotype, the male AROM + mice present with gynecomastia and severe disorders in their reproductive organs [8,9]. The hormonal levels and consequently the feminized phenotype in the AROM + males are normalized after aromatase inhibitor treatment [10]. Thus, the AROM + mouse model is a suitable tool to study the consequences of increased estrogen exposure in males in the context of reduced levels of androgens.

The aim of the present study was to understand how an increase in E/A regulates liver lipid metabolism in males. In this work, the effect of high circulating estrogen-to-androgen ratio (E/A) on liver proteome and transcriptome, and consequently on plasma phospholipid profile, was studied by a combination of LC–MS label free proteomics, mRNA microarray and phospholipid profiling by LC–MS/MS. We show that high E/A in male mice is linked to higher peroxisomal β-oxidation and lower arachidonic acid (AA) metabolism in the liver, and consequently to altered plasma phospholipid profile. In this context it is also interesting to note that altered plasma phospholipid profile has been recently linked to several diseases, such as hepatocellular carcinoma and liver cirrhosis [11] and type 1 diabetes [12]. The results of this study demonstrate that plasma phospholipid profiling provides specific information on lipid metabolism in the liver and could be used as a marker for liver steatosis and other metabolic disorders.

2. Materials and methods

2.1. Mouse model

The AROM + transgenic mouse model has been described previously [8]. Mice aged between 14 and 18 weeks were used for the proteomics, transcriptomics and metabolomics analyses. The mice were given soy-free natural ingredient feed (Special Diets Services, Witham, UK) and tap water ad libitum, and housed in specific pathogen-free conditions at Central Animal Laboratory, University of Turku, complying with international guidelines on the care and use of laboratory animals. Animal handling was conducted in accordance with Finnish Animal Ethics Committee and the institutional animal care policies of the University of Turku (Turku, Finland), which fully meet the requirements as defined in the NIH Guide on animal experimentation (NIH publication 86-23). For screening the general bioenergetics parameters, animals were shipped to the German Mouse Clinic (GMC) and maintained in IVC cages according to GMC housing conditions and German laws. All tests performed at the GMC were approved by the responsible authority of the government of Upper Bavaria. The GMC screen comprises extensive, standardized phenotyping of mice between the age of 9 and 21 weeks [13]. To confirm the altered sex steroid concentrations between AROM + and wild type (WT) mice serum, the concentrations of estradiol (E2), estrone (E1), testosterone (T) and androstenedione (A-dione) were analyzed in a single run by validated gas chromatography tandem mass spectrometry method [14]. The analyzed mice were at the age of 2 months.

2.2. Proteomics

Liver samples of seven WT and five AROM + male mice were prepared as described previously by Kanerva and coworkers [15] with minor modifications: The samples were homogenized in the presence of complete Mini EDTA-free Protease Inhibitor Cocktail (Roche, Basel, Switzerland) and the protein concentration was measured by DC Assay (Biorad). The proteins were precipitated by acetone and subjected to trypsin digestion with the trypsin–protein ratio of 1/60. The samples were analyzed on an LTQ Orbitrap Velos Pro mass spectrometer coupled to an EASY-nLC liquid chromatography system (Thermo Scientific). Sample loading, solvent delivery and scan functions were controlled by Xcalibur software (v2.1.0 SP1.1160; Thermo Scientific).

The 12 mouse liver peptide samples were injected in a randomized order and a combined sample consisting of equal amount of peptides from each liver sample was injected four times at regular intervals (Fig. 1). An amount of 200 ng of peptides, as estimated by the measurement of the absorbance at 280 nm by Nanodrop ND-1000 spectrophotometer (version 3.7.1, Thermo Fisher Scientific), was used in each injection. Peptide elution was accomplished by a 95 min long gradient from 98% solvent A (98% H_2O, 2% ACN and 0.2% HCOOH) to 35% solvent B (95% ACN, 5% H_2O and 0.2% HCOOH) with a flow rate 0.3 μl/min. Peptides were subjected to reversed-phase separation by a 2.5 cm long, 75 μm inner diameter trap column, and a 15 cm long, 75 μm inner diameter, analytical column packed in-house with C18 particles (Magic AQ C18 resin — 5 μm/200 Å, Bruker-Michrom, Billerica, MA, USA).

The Orbitrap mass analyzer was operated in a positive-ion mode in a mass range of 300–2000 m/z. A preview scan followed by a survey scan (MS1) at a resolution of 60,000 was executed in each cycle. Precursor ions were selected for fragmentation (MS/MS) by collision induced dissociation (CID) in the ion trap mass analyzer, after which they were added to an exclusion list for 60 s. The 12 mouse liver peptide samples and the first injection of the combined sample were analyzed in Orbitrap Velos Pro in Data Dependent Acquisition (DDA) mode, where the 15 most intense doubly or triply charged parent masses were automatically selected for fragmentation (Fig. 1).

Combined sample was injected at regular intervals to monitor the technical performance of the liquid chromatography and MS1-level quantification throughout the sample series. However, to minimize the redundancy in the precursor ion identifications (MS/MS-level) for the combined sample, a directed proteomics approach was chosen [16,17]. Therefore, the injections 2–4 of the combined sample were analyzed by only fragmenting the precursors that were not identified in the previous injections of the sample (Fig. 1). This was accomplished by the construction of inclusion lists consisting of unidentified and unfragmented precursor ion masses by Progenesis 4.0 (Nonlinear Dynamics, Newcastle upon Tyne, UK). In Progenesis the precursor ions were recognized by an automatic feature detection algorithm. An inclusion list was constructed containing those precursors (2 +, 3 +) that were eluted in a window of 6 s or more and were not identified in Mascot with at least two spectra per feature and mass error lower than 5 ppm. The variations in retention time were compensated by expanding the retention time window for each precursor by 1 min in the inclusion list.

The database searches were performed in Proteome Discoverer (v1.3.0.339; Thermo Scientific). Mascot algorithm (Matrix Science, London, UK) was used for the construction of inclusion lists for the combined peptide sample, whereas in the final collective search of all 16 analyzed samples, both Mascot [18] and Sequest [19] were used. The spectra were searched against UniProtKB/Swiss-Prot mouse database (16,686 sequences, accessed 15th of February 2013), appended with protein contaminants from cRAP (the common Repository of Adventitious Proteins, accessed 3rd of March 2011). The data was searched for tryptic peptides with Percolator decoy search mode, allowing maximum two missed cleavage sites, 5 ppm precursor mass tolerance, 0.5 Da fragment mass tolerance and 1% FDR. Finally, those proteins fulfilling the inclusion criteria of having at least two peptide spectral matches and at least one unique identified peptide were exported to Progenesis for quantification.

Spectral data from the 16 mass spectrometry runs were imported to Progenesis 4.0 for feature detection and data analysis. All LC–MS maps were aligned to the second injection of the combined sample and the feature detection was performed by automatic peak picking algorithm in default sensitivity mode. In peak picking, the maximum charge of precursor was restricted to 3 + and the retention time window to 12 s. The linear section of the gradient was used in the analysis and the threshold for accepted normalization was 0.5–1.75 within all peptide features. The contaminants and features that were identified by less than two hits or had precursor mass tolerance higher than

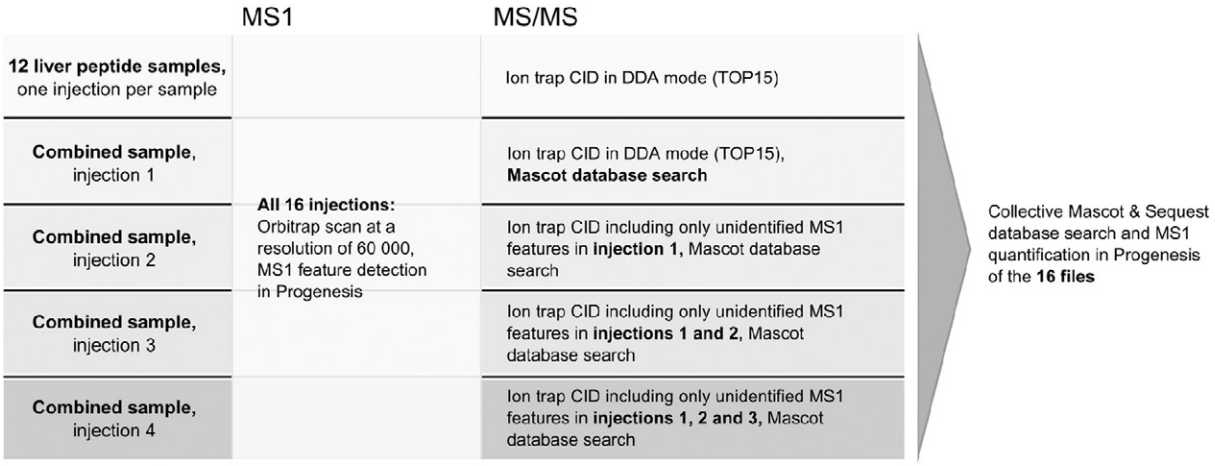

Fig. 1. Analysis schema used in the LTQ Orbitrap Velos Pro MS. The 16 files in the dataset include 12 injections of mouse liver peptide samples and four injections of a combined sample consisting of equal amounts of peptides from each liver sample. A common MS1 analysis scheme was used in all injections. In MS/MS, the 12 mouse liver peptide samples and the first injection of the combined sample were analyzed in DDA mode. In the injections 2–4 of the combined sample, only those precursors that were not identified in the previous injections of the combined sample were subjected to MS/MS. CID, collision induced dissociation; DDA, data dependent analysis.

5 ppm were removed. Significant differences in protein abundances between the AROM+ and WT mice were identified using the reproducibility optimized test statistic (ROTS); [20,21]. Proteins with FDR < 0.05 were defined as changed. The statistical workflow was optimized and described in detail earlier [22].

2.3. RNA isolation and microarray

Gene expression profiles in the liver of male AROM+ and WT mice were compared by microarray analysis, which was carried out at the Finnish DNA Microarray and Sequencing Centre, Turku Centre for Biotechnology. Total RNA was isolated from three WT and three AROM+ liver tissues using TRIsure reagent according to the manufacturer's instructions (Bioline reagents, London, UK). Three micrograms of total RNA were treated with deoxyribonuclease I (DNase I Amplification Grade Kit; Invitrogen Life Technologies, Paisley, UK), subsequently purified using the NucleoSpin® RNA XS kit (Marcherey-Nagel, Düren, Germany) and used to probe MouseWG-6 v2.0 Expression BeadChip microarray (Illumina, Essex, UK) according to protocols provided by the manufacturer. Differentially expressed genes were identified using Limma-package of the statistical software R (http://r-project.org). The level of statistical significance was set at FDR < 0.05 and fold change >2 to limit the number of up- or down-regulated genes.

2.4. Quantitative real-time RT-PCR (qRT-PCR)

Reverse transcription PCR was carried out by using the DyNAmo cDNA synthesis kit (Thermo Scientific, Waltham, MA, USA) and the quantitative PCR by using the DyNAmo Flash SYBR Green qPCR kit (Thermo Scientific). Triplicate samples of AROM+ and WT male livers were analyzed and statistical significances (p-values) were determined by unpaired *t*-test. Primer sequences and qRT-PCR conditions for analyzing the expression of peroxisomal 3-ketoacyl-CoA thiolase B (Acaa1b), acyl-CoA thioesterases (Acot) 3 and 4, cytochrome P450 4A12A (Cyp4a12a), peroxisomal bifunctional enzyme (Ehhadh), peroxisomal coenzyme A diphosphatase (Nudt7) and non-specific lipid-transfer protein 2 (Scp2) are described in Supplementary Table 1. L19 and Ppia were used as endogenous controls. We confirmed by the transcriptomic data that the expression of these genes was not altered in mouse liver in our study setup. In Illumina array, the expression levels were normalized with a quantile method, and the fold changes and FDR values were the following: L19 (=Rpl19): FC 1.079 and FDR 0.92; PPia (the first probe): FC 1.027 and FDR 0.96; PPia (the second probe): FC 1.071 and FDR 0.88.

2.5. Pathway analysis and correlation studies

The lists of quantified proteins and mRNAs were imported to Ingenuity Pathway Analysis system (IPA; Ingenuity® Systems, www.ingenuity.com, version: 24390178, 2015-06-17). The pathway analysis was performed with following settings: Direct and indirect experimentally observed relationships and endogenous chemicals were included in the analysis. Briefly, the pathways recognized in the quantitative proteomics and transcriptomics data were superimposed to all pathways found in the IPA and the significance of enrichment was calculated by Fisher's exact test. The protein and mRNA fold changes were log2 transformed and analyzed with Pearson correlation method with linear regression (GraphPad Prism 6.01).

2.6. Metabolomics

The metabolites were measured in the plasma of 26 (13 WT, 13 AROM+) male mice using Absolute*IDQ*TM p150 kit (BIOCRATES Life Sciences, Innsbruck, Austria) according to the instructions provided by the manufacturer. The assay allows simultaneous quantification of 163 metabolites out of 10 μl plasma, and includes free carnitine, 40 acylcarnitines (Cx:y), 14 amino acids (13 proteinogenic + ornithine), hexoses (sum of hexoses — about 90–95% glucose), 92 glycerophospholipids (15 lysophosphatidylcholines (lysoPC) and 77 phosphatidylcholines (PC)), and 15 sphingolipids (SMx:y). The abbreviations Cx:y are used to denominate the total number of carbons and double bonds of all chains, respectively (for more details see Ref [23]). The method of Absolute*IDQ*TM p150 kit has been proven to be in conformance with FDA-Guideline "Guidance for Industry — Bioanalytical Method Validation (May 2001"), which implies proof of reproducibility within a given error range. The assay procedures of the kit as well as the metabolite nomenclature have been described in detail in our previous work. Furthermore, the implementation of standardized quality assurance has been previously shown by us [23,24].

In short: For each sample, 10 μl of plasma were applied onto filters inserted in a 96 well sandwich plate, which already contained stable isotope labeled internal standards. The filters were dried in a stream of nitrogen; amino acids were derived with 5% phenylisothiocyanate reagent (PITC) and filters were dried again. Metabolites and internal standards were extracted using 5 mM ammonium acetate in methanol and the resulting solution was centrifuged through the filter membrane. After dilution with MS running solvent, final extracts were analyzed by flow injection analysis (FIA)–MS/MS. Sample handling was performed

by a Hamilton Microlab STARTM robot (Hamilton Bonaduz AG, Bonaduz, Switzerland) and an Ultravap nitrogen evaporator (Porvair Sciences, Leatherhead, U.K.), beside standard laboratory equipment. Mass spectrometric analyses were performed on an API 4000 triple quadrupole system (Sciex, Darmstadt, Germany) equipped with a 1200 Series HPLC (Agilent Technologies, Böblingen, Germany) controlled by the software Analyst 1.6.1. Data evaluation for quantification and quality assessment was performed with the Met*IDQ*TM software package. Using internal standards as a reference, the metabolite concentrations [μM] were calculated and log-transformed before statistical testing. Metabolites with significantly different concentrations between AROM+ and WT mice were identified using linear regression models implemented in the statistical software R. Concentration differences were considered to be significant for FDR < 0.05.

3. Results

3.1. Protein and gene expression patterns in the male mouse liver are altered by the increased estrogen-to-androgen ratio

The proteome study clearly indicated differential abundances of peptide ions between AROM+ and WT male liver. On average 7606 peptide features were identified in the 12 samples analyzed (7 WT and 5 AROM+) with the median technical coefficient of variance of 10% as calculated from the repeated injections of the combined sample. In the first injection of the combined sample, 2762 peptide features with two or more peptide spectrum matches (PSMs) were identified. Using the directed approach, additional 790, 146 and 303 peptides with two or more PSMs were identified based on the second, third and fourth injection, respectively (Fig. 2A). The amount of unspecific identifications (redundant peptide features) was decreasing at each inclusion round from 1397 to 473 and to 191 (Fig. 2B). Altogether, 1451 proteins were assigned with unique peptides and used for quantitation. In a hierarchical clustering analysis of these proteins, AROM+ and WT liver samples were clearly in distinct clusters (Fig. 3A). Furthermore, 166 proteins indicated differential abundances of peptide ions between the sample groups (FDR < 0.05; Supplementary Table 2).

Microarray analysis for the mRNA expression further confirmed the differential expression pattern of the mRNAs in AROM+ male mouse liver as compared with WT. Accordingly with the proteome study, in the hierarchical clustering analysis of the microarray data, separate groups of WT and AROM+ samples were formed (Fig. 3B). Furthermore, the correlation values within the groups were high, indicating small sample-to-sample differences. Based on the microarray a total of 159 genes were differently expressed between WT and AROM+ mice (FDR < 0.05, fold change >2; Supplementary Table 3).

As the complete proteomics and transcriptomics datasets were compared, a modest correlation of $R^2 = 0.54$ was found (Fig. 3D). Post transcriptional, translational or protein degradation regulation further increased the difference between AROM+ and WT for most of the differentially expressed genes. However, only for few genes, such as Cyp4a12a, Cyp2d9 and A1bg, the fold was higher in the transcriptomics than in the proteomics data (Supplementary Tables 2 and 3).

3.2. The expression of lipid metabolism related genes is deregulated in the liver of AROM+ males

The pathway analysis was performed to detect the impact of the increased E/A in the murine liver. In the analysis, the fatty acid metabolism (p-value 1.78E-06 for mRNA, 1.78E-11 for proteins) and

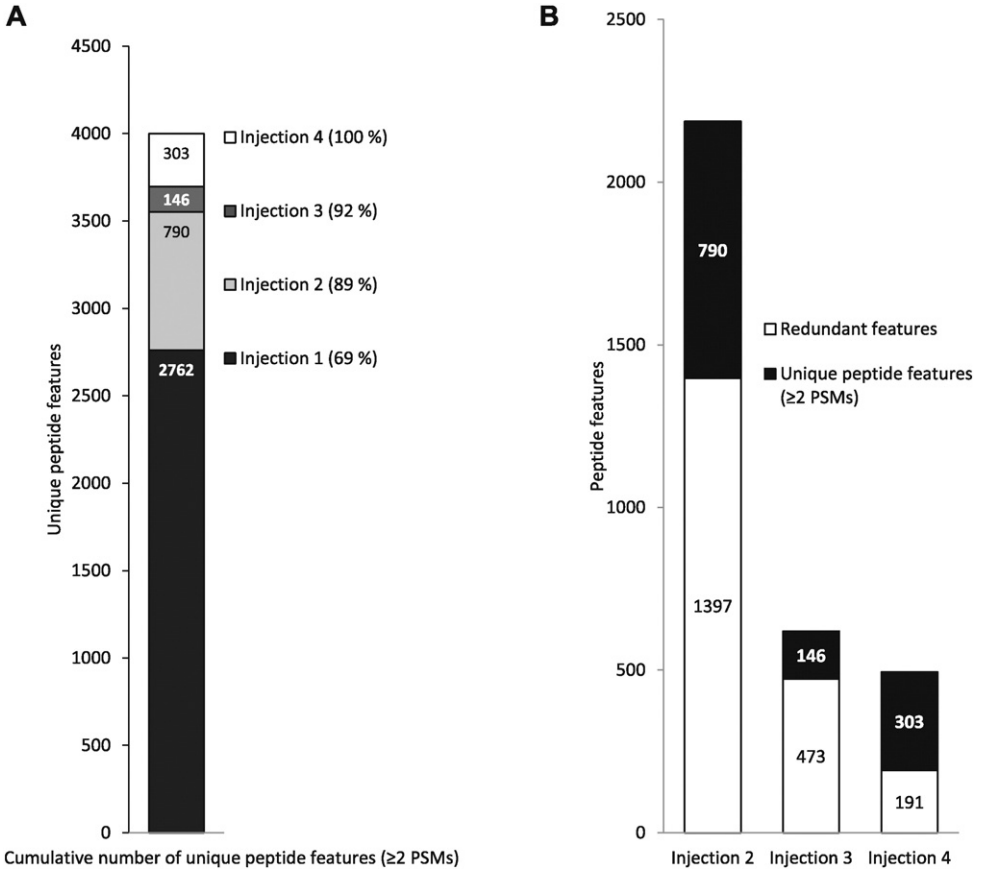

Fig. 2. The number of peptide features identified and inclusion specificity by the directed proteomics approach. The approach resulted in a cumulative increase of 45% of identified peptide features with two or more peptide spectrum matches (PSMs) (A). The relative amount of unique peptides was increasing with the decreasing amounts of precursor ions in the inclusion list (B).

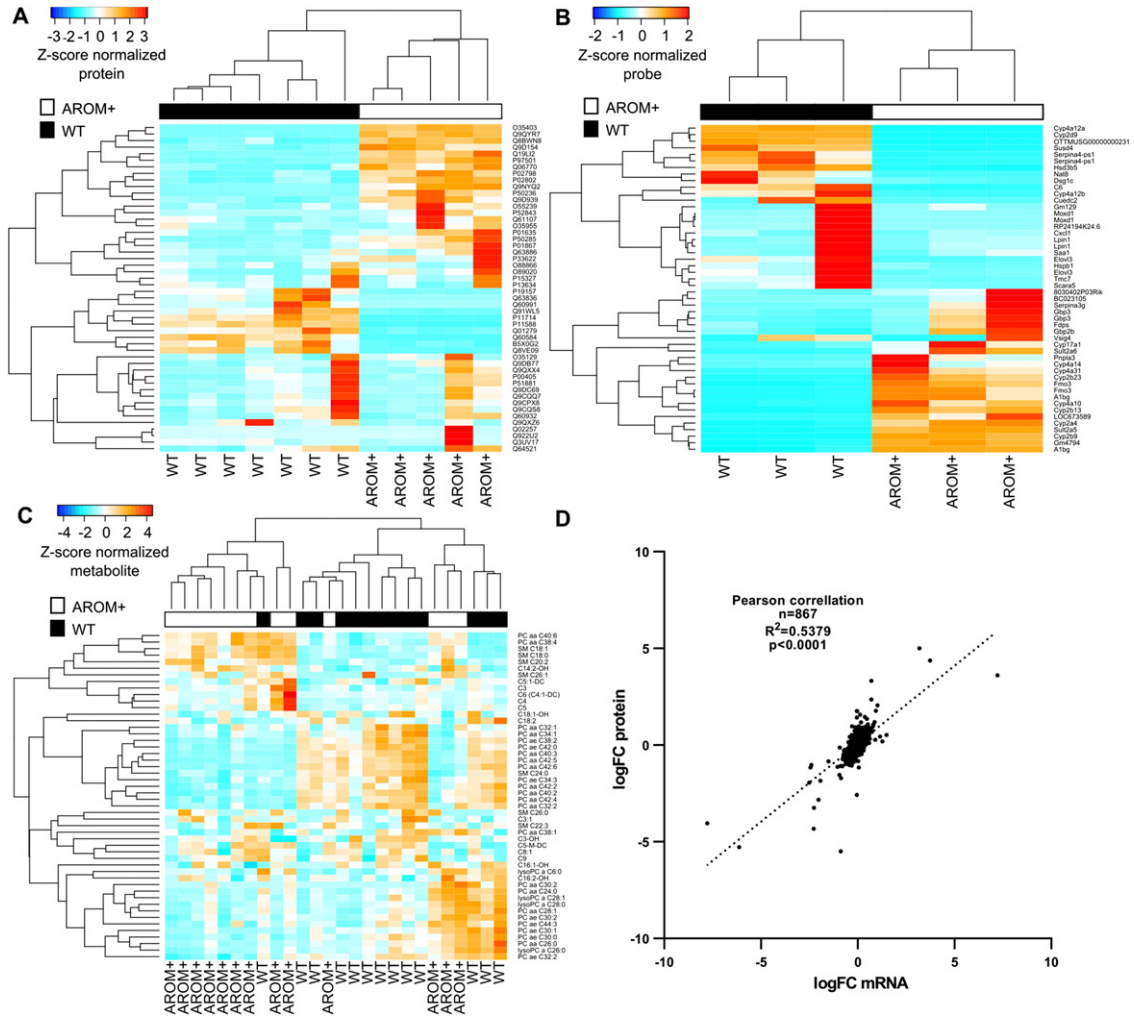

Fig. 3. Hierarchical clustering of omics data and the correlation of protein and transcript level data. Hierarchical clustering analyses of the omics datasets show clear differences in the liver protein and gene expression profile and in the plasma metabolite composition between AROM+ and WT males in proteomics (A), mRNA (B) and metabolomics (C) datasets. The measurements were filtered to top 50 features based on coefficients of variation and the remaining features were z-score normalized and processed using complete linkage hierarchical clustering of the Euclidean distances. A Pearson correlation plot was generated for comparison of protein and mRNA fold change values after log2 transformation (D).

metabolism of terpenoid (p-value 5.62E-07 for mRNA, 1.86E-12 for proteins) were enriched in both proteomics and transcriptomics datasets. In addition, the pathways of metabolism of acyl-coenzyme A (p-value 5.08E-13), oxidation of lipid (p-value 9.44E-12), conversion of lipid (p-value 1.49E-11) and concentration of lipids (p-value 1.50E-09) were highly enriched in protein data, and steroid metabolism (p-value 2.10E-06), hydroxylation of lipid (p-value 3.79E-06) and hydroxylation of eicosanoid (p-value 7.95E-06) among other pathways were highly enriched in mRNA data (Table 1A). Nuclear receptors PPARα (peroxisome proliferator-activated receptor alpha), RORα (retinoic acid receptor-related orphan receptor alpha) and NR1I2 (nuclear receptor subfamily 1 group I member 2), and ligands for PPARα, namely ciprofibrate and pirinixic acid, were listed as activated upstream regulators by IPA, whereas an inhibition of Acox1 (peroxisomal acyl-coenzyme A oxidase 1) enzyme was predicted (Table 1B).

Specifically, deregulation of genes related to peroxisomal β-oxidation was identified. Significant up-regulation of Ehhadh and Acaa1b, enzymes involved in the classical β-oxidation pathway [25,26], was detected in proteomics data (Fig. 4A). This finding was confirmed by qRT-PCR that revealed significant up-regulation of Ehhadh and tendency for up-regulation of the expression of Acaa1b gene (Fig. 4B). In addition, the expression of acyl-CoA thioesterases, Acot3 and Acot4 [27], was significantly up-regulated both at mRNA and protein levels (Fig. 4A–B), while the expression of Nudt7, a coenzyme A diphosphatase [28], was significantly down-regulated in both proteomics and qRT-PCR analyses (Fig. 4A–B). In contrast to the enzymes in the classical β-oxidation pathway, the expression of Scp2, a thiolase cleaving branched fatty acids and fatty dicarboxylic acids (DCAs) in the non-inducible β-oxidation pathway [29], was down-regulated both at protein and mRNA levels in the liver of AROM+ as compared with WT mice (Fig. 4A–B).

Interestingly, the expression of a male specific Cyp4a12a gene, which catalyzes ω-oxidation reactions in the smooth endoplasmic reticulum and specifically hydroxylates arachidonic acid (AA) to 20-hydroxy AA (20-HETE) [30,31], was dramatically down-regulated at protein and mRNA levels (Fig. 4A–B). Moreover, male specific Cyp2d9 protein and mRNA levels were lower, whereas female specific A1bg protein and mRNA levels, and Cyp2b9 and Cyp2b13 mRNA levels were higher in the liver of AROM+ males as compared with WT males (Supplementary Tables 2 and 3).

3.3. AROM+ male mice have a special pattern of phospholipids in the plasma

Similarly to the microarray and proteome analyses, AROM+ and WT males mainly clustered into different groups in the hierarchical clustering analysis of 163 plasma metabolites (Fig. 3C). Statistical evaluation of the results revealed 62 metabolites with significantly different

(FDR < 0.05) concentrations in AROM+ plasma as compared with the WT males. These metabolites included hexose, three amino acids, six acylcarnitines, 10 sphingomyelins, 38 phosphatidylcholines and four lysophosphatidylcholines. Metabolites showing the most significant changes are shown in Fig. 5, and all metabolomics results are presented in Supplementary Table 4. The metabolites decreased in AROM+ plasma (Fig. 5A) consist mostly of long chain diacyl (aa) and acyl–alkyl (ae) phosphatidylcholines (PC), with an exception of sphingomyelin (SM) 24:0. The decreased concentration of long chain phospholipids (PLs) is consistent with our observations on the increased expression of peroxisomal β-oxidation genes in AROM+ liver. The metabolites showing increased concentrations in AROM+ plasma form a more heterogeneous group, including: $PC_{aa}C38:4$, $PC_{ae}38:4$ and $PC_{aa}C40:6$, lysoPC(18:0) and lysoPC(20:4) and SMs, amino acids, such as arginine, and short chain acylcarnitines C3 and C4 (Fig. 5B). Interestingly, AA (C20:4) was one of the fatty acids present in the increased PLs, as probably the most abundant compositions of $PC_{aa}C38:4$ and $PC_{ae}38:4$ are PC(18:0/20:4) or PC(20:4/18:0). Thus, the increased amount of these PLs in plasma is in line with the dramatic down regulation of the expression of Cyp4a12a gene in the liver.

3.4. General bioenergetics parameters and steroid hormone levels in AROM+ male mice

Increased peroxisomal β-oxidation or decreased ω-oxidation in the liver had no effects on other metabolic parameters (body weight, food consumption, rectal temperature, daily feces production, energy uptake, energy content of the feces, metabolizable energy and the food assimilation coefficient) investigated in the primary phenotyping analysis of the German Mouse Clinic [13,32] (Supplementary Table 5). Consistent with our previous report [10], we found significantly lower T and higher E2 concentrations in the serum of AROM+ (T, 385 ± 58 pg/ml; E2, 30.9 ± 18.4 pg/ml) mice as compared with WT (T, 4972 ± 2067 pg/ml; E2, <0.3 pg/ml) males. In addition, A-dione concentrations (165 ± 21 pg/ml in AROM+; 180 ± 67 pg/ml in WT) were decreased

Table 1
Results of the Ingenuity pathway analysis. Ten most enriched pathways (A) and predicted upstream regulators (B) in the liver of AROM+ compared to WT.

A

Functions annotation	p-Value
mRNA microarray	
Complement component deficiency	3.82E-07
Metabolism of terpenoid	5.62E-07
Complement activation	1.55E-06
Fatty acid metabolism	1.78E-06
Steroid metabolism	2.10E-06
Hydrolysis of glycosylceramide	3.20E-06
Hydroxylation of lipid	3.79E-06
Metabolism of xenobiotic	4.79E-06
Accumulation of cells	6.11E-06
Hydroxylation of eicosanoid	7.95E-06
Proteomics	
Metabolism of acyl-coenzyme A	5.08E-13
Metabolism of terpenoid	1.86E-12
Metabolism of xenobiotic	2.88E-12
Oxidation of lipid	9.44E-12
Conversion of lipid	1.49E-11
Fatty acid metabolism	1.78E-11
Metabolism of amino acids	4.96E-10
Modification of retinaldehyde	7.73E-10
Metabolism of nucleic acid component or derivative	1.05E-09
Concentration of lipid	1.50E-09

B

Upstream regulator	Molecule type	Activation z-score (*Predicted Activation State*)	p-Value
mRNA microarray			
GPD1	Enzyme		4.30E-34
SLC25A13	Transporter		6.07E-34
NR1I2	Ligand-dependent nuclear receptor	1.942	1.26E-15
RORC	Ligand-dependent nuclear receptor		1.79E-15
PPARA	Ligand-dependent nuclear receptor	3.102 (*Activated*)	8.01E-15
RORA	Ligand-dependent nuclear receptor		2.34E-14
Ciprofibrate	Chemical drug	2.649 (*Activated*)	2.12E-13
Pirinixic acid	Chemical toxicant	3.257 (*Activated*)	2.89E-13
ACOX1	Enzyme	−2.741 (*Inhibited*)	4.05E-11
1,4-bis[2-(3,5-dichloropyridyloxy)]benzene	Chemical toxicant	1.071	5.14E-11
Proteomics			
PPARA	Ligand-dependent nuclear receptor	2.15 (*Activated*)	5.54E-21
ACOX1	Enzyme	−1.996	4.94E-20
TO-901317	Chemical reagent	1.151	3.66E-19
Ciprofibrate	Chemical drug	2.776 (*Activated*)	1.96E-18
Methylprednisolone	Chemical drug	−0.632	3.92E-18
Pirinixic acid	Chemical toxicant	0.634	6.10E-18
NR1I2	Ligand-dependent nuclear receptor	1.27	1.20E-15
RORA	Ligand-dependent nuclear receptor	1.96	3.14E-14
Dihydrotestosterone	Chemical-endogenous mammalian	0.941	3.52E-12
SREBF1	Transcription regulator	2.299 (*Activated*)	1.55E-11

p-Value indicates the overlap of genes or proteins in the data and genes or proteins regulated by the upstream regulator in the Ingenuity database.

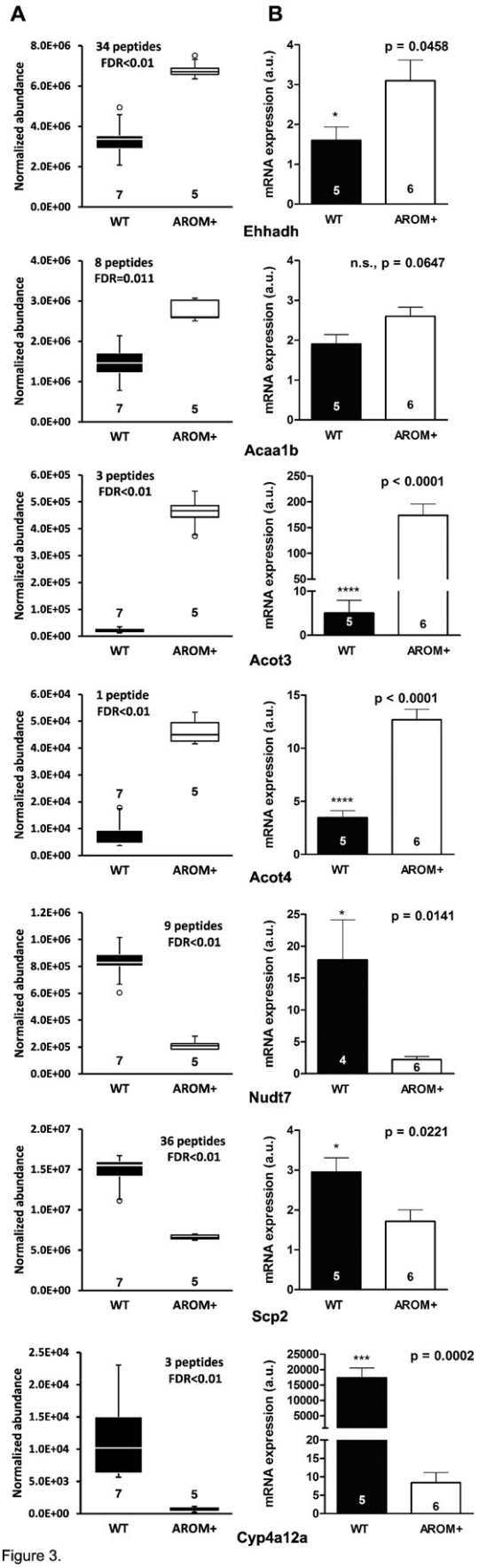

Figure 3.

and E1 increased (9.7 ± 0.7 pg/ml in AROM+; <0.5 pg/ml in WT) in AROM+ males, although the changes were not significant.

4. Discussion

Estrogens have a wide range of effects on male health, including metabolism. In this study, we describe how an increased circulating E/A in male mice (AROM+ mouse model) is linked to changes in the liver lipid metabolism and consequently to phospholipid profile in the plasma.

The changes on proteome and transcriptome in AROM+ liver were studied by a pathway analysis. Several pathways related to lipid metabolism were listed in the ten mostly regulated ones. For example, the pathways regulating the metabolism of fatty acids and terpenoids were significantly altered in both mRNA and protein data sets. Furthermore, a modest correlation ($R^2 = 0.54$) was found between transcriptome and proteome, being in line with previous reports [33–36]. For most of the genes, regulatory processes downstream of transcription further increased the difference between AROM+ and WT mice.

In our data, we specifically observed increased expression of genes related to peroxisomal fatty acid β-oxidation in AROM+ liver. The β-oxidation in the rodent peroxisomes can be divided into the classical PPARα-inducible system oxidizing very long (>C20) and long (C14–C20) fatty acid CoAs, and to the non-inducible system oxidizing branched lipids and fatty dicarboxylic acids (DCAs) [37,38]. Interestingly, we observed an induction of the classical PPARα-regulated β-oxidation pathway, characterized by increased expression of Ehhadh and Acaa1b enzymes [39,40]. Moreover, the expression of Acot3 and Acot4, PPARα regulated peroxisomal proteins that produce small acyl-CoAs for mitochondrial β-oxidation at the final steps of peroxisomal reactions [27,41], was upregulated. Conversely, we observed a decrease in the expression of Scp2 gene, which indicates a possible down regulation of the non-inducible pathway in AROM+ liver [29,42]. In addition, Nudt7, an enzyme terminating the peroxisomal β-oxidation, has been shown to be down regulated by PPARα, which is consistent with our results [28].

Consistently, pathway analysis indicated PPARα and its ligands ciprofibrate and pirinixic acid as upstream regulators. Furthermore, the pathway analysis provided evidence for the activation of retinoic acid receptor-related orphan receptor alpha (RORα) upstream of deregulated genes. Interestingly, RORα has been recently shown to regulate PPARα expression in the liver [43], and estrogens and androgens activate and suppress, respectively, the expression of RORα in human neuronal cells [44]. Our findings are in line with previous studies showing interplay between PPARα and E2 [45–48]. In an agreement with our study, Fernández-Pérez and coworkers recently demonstrated that in hypothyroid-orchidectomized male rats E2 induced expression of PPARα and PPARα target genes involved in liver β- and ω-oxidation [49]. Furthermore, Nemoto and coworkers [6] showed a decreased β-oxidation both in mitochondria and peroxisomes in the liver of aromatase deficient male ArKO mice. Intolerance in glucose homeostasis preceded the imbalanced lipid metabolism in the liver of male ArKO mice, and combined roles of both estrogens and glucose homeostasis were suggested in the development of hepatic steatosis [7].

The role of estrogen receptors (ERs) in the liver function has been previously studied in other genetically modified mouse models. Bryzgalova and coworkers [50] showed with ERα and ERβ knockout models (ERαKOs and ERβKOs) that ERα regulates liver glucose homeostasis and the expression of lipogenic genes in a gender-independent manner. A recent study with mouse model expressing ERα exclusively in the plasma membrane (MOER mouse) indicates that the expression of lipid synthesis-related genes is controlled by membrane-bound, not

Fig. 4. Proteomics data are consistent with quantitative (q) RT-PCR results. The left column (A) shows the protein expression of the indicated genes measured by quantitative proteomics analysis (FDR determined by ROTS) and the right column (B) corresponding qRT-PCR results (p-values assessed by unpaired *t*-test) for WT and AROM+ male livers.

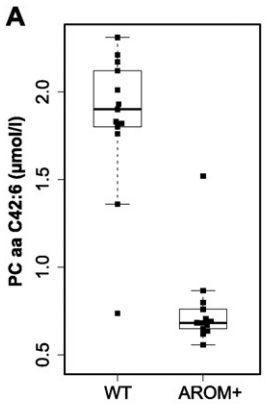

metabolite	b-value (AROM+)	FDR
PC_{aa}42:6	**-0.39**	**1.3E-06**
PC_{aa}40:3	-0.45	2.6E-06
PC_{ae}38:2	-0.25	2.7E-06
PC_{aa}42:5	-0.33	6.0E-06
PC_{ae}42:0	-0.23	2.5E-05
SM (24:0)	-0.23	2.5E-05
PC_{aa}40:4	-0.18	3.9E-05
PC_{aa}42:2	-0.23	4.6E-05
PC_{aa}40:2	-0.26	7.6E-05
PC_{ae}34:3	-0.18	0.00011
PC_{ae}36:2	-0.11	0.00018
PC_{aa}42:4	-0.20	0.00018
PC_{ae}34:2	-0.15	0.00020
PC_{ae}36:3	-0.15	0.00022
PC_{ae}36:1	-0.14	0.00034
PC_{aa}40:1	-0.14	0.00038
PC_{ae}38:6	-0.10	0.00068
PC_{ae}38:1	-0.15	0.0016

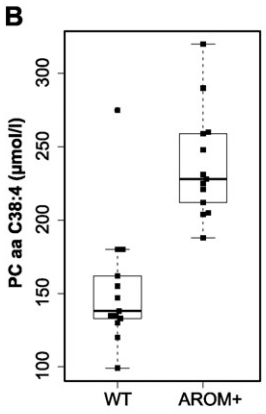

metabolite	b-value (AROM+)	FDR
SM (18:0)	0.34	3.9E-05
PC_{aa}38:4	**0.20**	**4.7E-05**
PC_{aa}40:6	0.18	0.00018
SM (18:1)	0.20	0.00046
Arg	0.14	0.0013
lysoPC(18:0)	0.13	0.0015
Trp	0.07	0.0022
SM (20:2)	0.57	0.0022
lysoPC (20:4)	0.12	0.0027
Thr	0.13	0.0032
SM (OH) (14:1)	0.09	0.018
SM (OH) (16:1)	0.09	0.020
PC_{ae}38:4	0.06	0.020
SM (OH) (24:1)	0.11	0.020
C3	0.12	0.026
C14:2-OH	0.11	0.041
SM (16:0)	0.06	0.041
C4	0.22	0.046

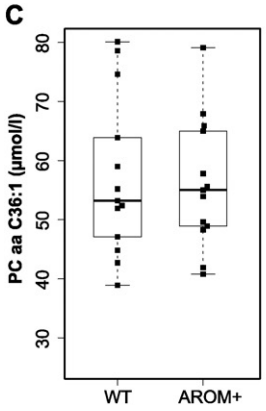

metabolite	b-value (AROM+)	FDR
Tyr	-0.013	0.41
SM (22:3)	-0.040	0.41
PC_{aa}36:2	-0.0063	0.41
PC_{aa}36:4	0.0065	0.41
C8:1	-0.013	0.42
C10	-0.0062	0.45
C8	0.0043	0.45
PC_{aa}36:5	0.0056	0.45
C3:1	-0.013	0.45
C9	-0.0069	0.46
PC_{ae}30:1	-0.026	0.46
PC_{aa}36:1	**-0.0041**	**0.46**
PC_{ae}36:5	0.0013	0.47
lysoPC (6:0)	0.0060	0.47
PC_{aa}24:0	-0.0049	0.47
PC_{ae}40:6	-0.00051	0.48
C5:1-DC	0.0017	0.48
C5-M-DC	-4.2E-05	0.48

Fig. 5. The comparison of metabolite changes in WT and AROM+ males. The metabolites showing decreased (A) or increased (B) amounts in the plasma are shown. In the third group (C), the amount of the metabolites was not changed. FDR and beta values were determined by linear regression analysis.

by nuclear ERα [51]. In line with this, hepatic insulin resistance reported in total ERKO mouse, was not observed in the mice with liver-selective nuclear ERα deficiency (LERKO) [52]. In the AROM+ mouse model, the effects in the liver might be regulated, in addition to ERs, by androgen receptor (AR), as the circulating androgen levels in AROM+ mice are low [8]. However, the role of AR in the increased β-oxidation in AROM+ mice is unlikely, as hepatic AR-knockout male mouse (H-AR-/y) develops liver steatosis and insulin resistance during aging and after high-fat diet [53].

The increased expression of the peroxisomal β-oxidation genes in the liver is in agreement with the decrease in plasma PL levels in AROM+ mice. Especially, the decreased concentrations of long chain PC aa and PC ae lipids refer to increased peroxisomal β-oxidation. As both aa and ae PCs are affected, the reduced levels are a result of decreased fatty acid concentrations prior to the plasmalogen synthesis preceding alkylglycerone phosphate synthase activity [54]. Additionally, the increased amount of short chain acylcarnitines C3 and C4 could be a result of increased expression of Acot3 and Acot4, which produce small acyl-CoAs. Moreover, the mitochondrial β-oxidation driven by carnitine palmitoyltransferase I was not affected as the acylcarnitines-free carnitines ratio (C2 + C3)/C0 was unaltered [55–57]. The previous study in rats showing a close correlation between phospholipid profile in the liver and plasma is in line with our finding that alterations in the liver lipid metabolism can be detected in the plasma [58].

In contrast to the reduction in the other long-chain plasma phospholipids, we observed increased amounts of abundant phospholipids PC_{aa}C38:4 and PC_{ae}C38:4 and their downstream metabolites in AROM+ mice plasma. The result indicates an increase in common phospholipid derived fatty acids such as stearic acid (C18:0) and AA (C20:4) in the circulation [59,60]. As AA is a well-known precursor of proinflammatory eicosanoids such as prostaglandins [61] and the biosynthesis of these molecules is dependent on its availability, the high level of AA in the plasma is of special interest. In line with plasma phospholipid levels, genes related to lipid and AA metabolism were deregulated in the liver of AROM+ mice. The most dramatic effect was the downregulation of Cyp4a12a (−16.4 and −219.6 fold at protein and mRNA levels, respectively), an enzyme responsible for hydroxylating free AA to 20-HETE and corresponding DCA in the liver ω-oxidation [30,31]. Thus, the decreased activity of the enzyme may increase the levels of circulating AA and decrease the amounts of DCA available for alternative pathway in peroxisomal β-oxidation. The decreased amount of DCA may in turn downregulate the expression of Scp2 in the AROM+ liver.

Interestingly, according to our data, the regulation of gene expression in the liver of AROM+ males is partially feminized. While strongly down regulated in AROM+ male liver, the Cyp4a12a and Cyp2d9 are typically highly expressed in male mice [30,62–64]. Furthermore, the expression of female-specific Cyp2b9, Cyp2b13 and A1bg genes [65,66] was up-regulated in the liver of AROM+ males both at the level of mRNA and protein. Unlike the several other genes studied, the genes involved in the gender specific liver function appear to be especially transcriptionally regulated.

5. Conclusion

In summary, our findings indicate a PPARα-mediated increase in the peroxisomal β-oxidation of very long and long chain fatty acids, and a deficient ω-oxidation of AA in the liver of male mice having increased circulating E2 and decreased T levels. Interestingly, the changes in the liver lipid metabolism are also associated with altered phospholipid profile in the plasma. Taken together, we suggest that an increased circulating E/A in males, on the one hand, has beneficial effects on lipid metabolism by increasing liver β-oxidation especially in the peroxisomes, and, on the other hand, decreases liver ω-oxidation offering more AA in the circulation.

Conflict of interest statement

The authors have nothing to disclosure regarding funding or conflict of interest concerning this manuscript.

Funding sources

This study was supported by Jalmari and Rauha Ahokas Foundation, Academy of Finland (project 128712), Sigrid Juselius Foundation and in part by a grant from the German Federal Ministry of Education, Research (BMBF) to the German Center for Diabetes Research (DZD e.V.) and the German Academic Exchange Service (DAAD). GMC researchers were funded by the German Federal Ministry of Education and Research

(Infrafrontier grant 01KX1012) and the German Center for Diabetes Research (DZD).

Transparency Document

The Transparency document associated with this article can be found, in online version.

Acknowledgments

We acknowledge the support from Turku Proteomics Facility of the Biocenter Finland Proteomics and Metabolomics infrastructure and Finnish National Doctoral Program in Informational and Structural Biology. We also thank Dr. Werner Roemisch-Margl, Julia Scarpa and Katharina Faschinger for support in metabolomics measurements performed at Helmholtz Zentrum München Genome Analysis Center, Metabolomics Core Facility. We thank the Finnish DNA Microarray and Sequencing Centre, Saira Afzal for the statistical proteomics analyses and Pekka Haapaniemi for excellent assistance in Turku Centre for Biotechnology. Katri Hovirinta, Heli Niittymäki, Nina Messner and Jonna Palmu in Turku Center for Disease Modeling are acknowledged for their skillful technical assistance.

Appendix A. Supplementary data

This material is available free of charge via the Internet at http://pubs.acs.org.Free.pdf viewer available at: http://get.adobe.com/uk/reader/. Supplementary data associated with this article can be found in the online version, at http://dx.doi.org/10.1016/j.jprot.2015.12.009.

References

[1] B.L. Herrmann, B. Saller, O.E. Janssen, P. Gocke, A. Bockisch, H. Sperling, et al., Impact of estrogen replacement therapy in a male with congenital aromatase deficiency caused by a novel mutation in the CYP19 gene, J. Clin. Endocrinol. Metab. 87 (2002) 5476–5484.
[2] R. Bouillon, M. Bex, D. Vanderschueren, S. Boonen, Estrogens are essential for male pubertal periosteal bone expansion, J. Clin. Endocrinol. Metab. 89 (2004) 6025–6029.
[3] L. Maffei, Y. Murata, V. Rochira, G. Tubert, C. Aranda, M. Vazquez, et al., Dysmetabolic syndrome in a man with a novel mutation of the aromatase gene: effects of testosterone, alendronate, and estradiol treatment, J. Clin. Endocrinol. Metab. 89 (2004) 61–70.
[4] L. Maffei, V. Rochira, L. Zirilli, P. Antunez, C. Aranda, B. Fabre, et al., A novel compound heterozygous mutation of the aromatase gene in an adult man: reinforced evidence on the relationship between congenital oestrogen deficiency, adiposity and the metabolic syndrome, Clin. Endocrinol. 67 (2007) 218–224.
[5] K.N. Hewitt, K. Pratis, M.E. Jones, E.R. Simpson, Estrogen replacement reverses the hepatic steatosis phenotype in the male aromatase knockout mouse, Endocrinology 145 (2004) 1842–1848.
[6] Y. Nemoto, K. Toda, M. Ono, K. Fujikawa-Adachi, T. Saibara, S. Onishi, et al., Altered expression of fatty acid-metabolizing enzymes in aromatase-deficient mice, J. Clin. Invest. 105 (2000) 1819–1825.
[7] M.L. Van Sinderen, G.R. Steinberg, S.B. Jørgensen, S.Q. To, K.C. Knower, C.D. Clyne, et al., Hepatic glucose intolerance precedes hepatic steatosis in the male aromatase knockout (ArKO) mouse, PLoS One 9 (2014), e87230.
[8] X. Li, E. Nokkala, W. Yan, T. Streng, N. Saarinen, A. Wärri, et al., Altered structure and function of reproductive organs in transgenic male mice overexpressing human aromatase, Endocrinology 142 (2001) 2435–2442.
[9] X. Li, A. Wärri, S. Mäkelä, T. Ahonen, T. Streng, R. Santti, et al., Mammary gland development in transgenic male mice expressing human P450 aromatase, Endocrinology 143 (2002) 4074–4083.
[10] X. Li, L. Strauss, S. Mäkelä, T. Streng, I. Huhtaniemi, R. Santti, et al., Multiple structural and functional abnormalities in the p450 aromatase expressing transgenic male mice are ameliorated by a p450 aromatase inhibitor, Am. J. Pathol. 164 (2004) 1039–1048.
[11] Y. Liu, Z. Hong, G. Tan, X. Dong, G. Yang, L. Zhao, et al., NMR and LC/MS-based global metabolomics to identify serum biomarkers differentiating hepatocellular carcinoma from liver cirrhosis, Int. J. Cancer 135 (2014) 658–668.
[12] D. La Torre, T. Seppänen-Laakso, H.E. Larsson, T. Hyötyläinen, S.A. Ivarsson, A. Lernmark, et al., Decreased cord–blood phospholipids in young age-at-onset type 1 diabetes, Diabetes 62 (2013) 3951–3956.
[13] H. Fuchs, V. Gailus-Durner, T. Adler, J.A. Aguilar-Pimentel, L. Becker, J. Calzada-Wack, et al., Mouse phenotyping, Methods 53 (2011) 120–135.
[14] M.E. Nilsson, L. Vandenput, Å. Tivesten, A.K. Norlén, M.K. Lagerquist, S.H. Windahl, et al., Measurement of a comprehensive sex steroid profile in rodent serum by high-sensitive gas chromatography–tandem mass spectrometry, Endocrinology 156 (2015) 2492–2502.
[15] M. Kanerva, A. Vehmas, M. Nikinmaa, K.A. Vuori, Spatial variation in transcript and protein abundance of Atlantic salmon during feeding migration in the Baltic sea, Environ. Sci. Technol. (2014).
[16] A. Schmidt, N. Gehlenborg, B. Bodenmiller, L.N. Mueller, D. Campbell, M. Mueller, et al., An integrated, directed mass spectrometric approach for in-depth characterization of complex peptide mixtures, Mol. Cell. Proteomics 7 (2008) 2138–2150.
[17] A.P. Vehmas, D. Muth-Pawlak, K. Huhtinen, T. Saloniemi-Heinonen, K. Jaakkola, T.D. Laajala, et al., Ovarian endometriosis signatures established through discovery and directed mass spectrometry analysis, J. Proteome Res. 13 (2014) 4983–4994.
[18] D.N. Perkins, D.J. Pappin, D.M. Creasy, J.S. Cottrell, Probability-based protein identification by searching sequence databases using mass spectrometry data, Electrophoresis 20 (1999) 3551–3567.
[19] J.K. Eng, A.L. McCormack, J.R. Yates, An approach to correlate tandem mass spectral data of peptides with amino acid sequences in a protein database, J. Am. Soc. Mass Spectrom. 5 (1994) 976–989.
[20] L.L. Elo, S. Filén, R. Lahesmaa, T. Aittokallio, Reproducibility-optimized test statistic for ranking genes in microarray studies, IEEE/ACM Trans. Comput. Biol. Bioinform. 5 (2008) 423–431.
[21] L.L. Elo, J. Hiissa, J. Tuimala, A. Kallio, E. Korpelainen, T. Aittokallio, Optimized detection of differential expression in global profiling experiments: case studies in clinical transcriptomic and quantitative proteomic datasets, Brief. Bioinform. 10 (2009) 547–555.
[22] A. Pursiheimo, A.P. Vehmas, S. Afzal, T. Suomi, T. Chand, L. Strauss, et al., Optimization of statistical methods impact on quantitative proteomics data, J. Proteome Res. (2015).
[23] W. Römisch-Margl, C. Prehn, R. Bogumil, C. Röhring, K. Suhre, J. Adamski, Procedure for tissue sample preparation and metabolite extraction for high-throughput targeted metabolomics, Metabolomics 8 (2012) 133–142.
[24] T. Illig, C. Gieger, G. Zhai, W. Römisch-Margl, R. Wang-Sattler, C. Prehn, et al., A genome-wide perspective of genetic variation in human metabolism, Nat. Genet. 42 (2010) 137–141.
[25] S.M. Houten, S. Denis, C.A. Argmann, Y. Jia, S. Ferdinandusse, J.K. Reddy, et al., Peroxisomal L-bifunctional enzyme (Ehhadh) is essential for the production of medium-chain dicarboxylic acids, J. Lipid Res. 53 (2012) 1296–1303.
[26] V.D. Antonenkov, P.P. Van Veldhoven, E. Waelkens, G.P. Mannaerts, Comparison of the stability and substrate specificity of purified peroxisomal 3-oxoacyl-CoA thiolases A and B from rat liver, Biochim. Biophys. Acta 1437 (1999) 136–141.
[27] M.C. Hunt, M.I. Siponen, S.E. Alexson, The emerging role of acyl-CoA thioesterases and acyltransferases in regulating peroxisomal lipid metabolism, Biochim. Biophys. Acta 2012 (1822) 1397–1410.
[28] S.J. Reilly, V. Tillander, R. Ofman, S.E. Alexson, M.C. Hunt, The nudix hydrolase 7 is an acyl-CoA diphosphatase involved in regulating peroxisomal coenzyme A homeostasis, J. Biochem. 144 (2008) 655–663.
[29] B.P. Atshaves, A.L. McIntosh, D. Landrock, H.R. Payne, J.T. Mackie, N. Maeda, et al., Effect of SCP-x gene ablation on branched-chain fatty acid metabolism, Am. J. Physiol. Gastrointest. Liver Physiol. 292 (2007) G939–G951.
[30] D.N. Muller, C. Schmidt, E. Barbosa-Sicard, M. Wellner, V. Gross, H. Hercule, et al., Mouse Cyp4a isoforms: enzymatic properties, gender- and strain-specific expression, and role in renal 20-hydroxyeicosatetraenoic acid formation, Biochem. J. 403 (2007) 109–118.
[31] C. Arnold, M. Markovic, K. Blossey, G. Wallukat, R. Fischer, R. Dechend, et al., Arachidonic acid-metabolizing cytochrome P450 enzymes are targets of {omega}-3 fatty acids, J. Biol. Chem. 285 (2010) 32720–32733.
[32] V. Gailus-Durner, H. Fuchs, L. Becker, I. Bolle, M. Brielmeier, J. Calzada-Wack, et al., Introducing the German mouse clinic: open access platform for standardized phenotyping, Nat. Methods 2 (2005) 403–404.
[33] A.R. de Sousa, L.O. Penalva, E.M. Marcotte, C. Vogel, Global signatures of protein and mRNA expression levels, Mol. BioSyst. 5 (2009) 1512–1526.
[34] A.I. Nesvizhskii, F.F. Roos, J. Grossmann, M. Vogelzang, J.S. Eddes, W. Gruissem, et al., Dynamic spectrum quality assessment and iterative computational analysis of shotgun proteomic data: toward more efficient identification of post-translational modifications, sequence polymorphisms, and novel peptides, Mol. Cell. Proteomics 5 (2006) 652–670.
[35] K. Ning, D. Fermin, A.I. Nesvizhskii, Comparative analysis of different label-free mass spectrometry based protein abundance estimates and their correlation with RNA-Seq gene expression data, J. Proteome Res. 11 (2012) 2261–2271.
[36] C. Vogel, E.M. Marcotte, Insights into the regulation of protein abundance from proteomic and transcriptomic analyses, Nat. Rev. Genet. 13 (2012) 227–232.
[37] J.K. Reddy, Nonalcoholic steatosis and steatohepatitis. III. Peroxisomal beta-oxidation, PPAR alpha, and steatohepatitis, Am. J. Physiol. Gastrointest. Liver Physiol. 281 (2001) G1333–G1339.
[38] G.P. Mannaerts, P.P. Van Veldhoven, M. Casteels, Peroxisomal lipid degradation via beta- and alpha-oxidation in mammals, Cell Biochem. Biophys. 32 (Spring 2000) 73–87.
[39] V. Nicolas-Frances, V.K. Dasari, E. Abruzzi, T. Osumi, N. Latruffe, The peroxisome proliferator response element (PPRE) present at positions −681/−669 in the rat liver 3-ketoacyl-CoA thiolase B gene functionally interacts differently with PPARalpha and HNF-4, Biochem. Biophys. Res. Commun. 269 (2000) 347–351.
[40] J.K. Reddy, S.K. Goel, M.R. Nemali, J.J. Carrino, T.G. Laffler, M.K. Reddy, et al., Transcription regulation of peroxisomal fatty acyl-CoA oxidase and enoyl-CoA hydratase/3-hydroxyacyl-CoA dehydrogenase in rat liver by peroxisome proliferators, Proc. Natl. Acad. Sci. U. S. A. 83 (1986) 1747–1751.

[41] M.C. Hunt, S.E. Nousiainen, M.K. Huttunen, K.E. Orii, L.T. Svensson, S.E. Alexson, Peroxisome proliferator-induced long chain acyl-CoA thioesterases comprise a highly conserved novel multi-gene family involved in lipid metabolism, J. Biol. Chem. 274 (1999) 34317–34326.
[42] D. Lopez, R.B. Irby, M.P. McLean, Peroxisome proliferator-activated receptor alpha induces rat sterol carrier protein x promoter activity through two peroxisome proliferator-response elements, Mol. Cell. Endocrinol. 205 (2003) 169–184.
[43] Y. Lu, X. Liu, Y. Jiao, X. Xiong, E. Wang, X. Wang, et al., Periostin promotes liver steatosis and hypertriglyceridemia through downregulation of PPARα, J. Clin. Invest. 124 (2014) 3501–3513.
[44] T. Sarachana, V.W. Hu, Differential recruitment of coregulators to the RORA promoter adds another layer of complexity to gene (dys) regulation by sex hormones in autism, Mol. Autism 4 (2013) 39.
[45] R.P. Barros, J. Gustafsson, Estrogen receptors and the metabolic network, Cell Metab. 14 (2011) 289–299.
[46] F. Djouadi, C.J. Weinheimer, J.E. Saffitz, C. Pitchford, J. Bastin, F.J. Gonzalez, et al., A gender-related defect in lipid metabolism and glucose homeostasis in peroxisome proliferator-activated receptor alpha-deficient mice, J. Clin. Invest. 102 (1998) 1083–1091.
[47] L. Zhu, W.C. Brown, Q. Cai, A. Krust, P. Chambon, O.P. McGuinness, et al., Estrogen treatment after ovariectomy protects against fatty liver and may improve pathway-selective insulin resistance, Diabetes 62 (2013) 424–434.
[48] H. Gao, G. Bryzgalova, E. Hedman, A. Khan, S. Efendic, J.A. Gustafsson, et al., Long-term administration of estradiol decreases expression of hepatic lipogenic genes and improves insulin sensitivity in ob/ob mice: a possible mechanism is through direct regulation of signal transducer and activator of transcription 3, Mol. Endocrinol. 20 (2006) 1287–1299.
[49] L. Fernández-Pérez, R. Santana-Farré, M. de Mirecki-Garrido, I. García, B. Guerra, C. Mateo-Díaz, et al., Lipid profiling and transcriptomic analysis reveals a functional interplay between estradiol and growth hormone in liver, PLoS One 9 (2014), e96305.
[50] G. Bryzgalova, H. Gao, B. Ahren, J.R. Zierath, D. Galuska, T.L. Steiler, et al., Evidence that oestrogen receptor-alpha plays an important role in the regulation of glucose homeostasis in mice: insulin sensitivity in the liver, Diabetologia 49 (2006) 588–597.
[51] A. Pedram, M. Razandi, F. O'Mahony, H. Harvey, B.J. Harvey, E.R. Levin, Estrogen reduces lipid content in the liver exclusively from membrane receptor signaling, Sci. Signal. 6 (2013) ra36.
[52] M. Matic, G. Bryzgalova, H. Gao, P. Antonson, P. Humire, Y. Omoto, et al., Estrogen signalling and the metabolic syndrome: targeting the hepatic estrogen receptor alpha action, PLoS One 8 (2013), e57458.
[53] H.Y. Lin, I.C. Yu, R.S. Wang, Y.T. Chen, N.C. Liu, S. Altuwaijri, et al., Increased hepatic steatosis and insulin resistance in mice lacking hepatic androgen receptor, Hepatology 47 (2008) 1924–1935.
[54] R. Wang-Sattler, Y. Yu, K. Mittelstrass, E. Lattka, E. Altmaier, C. Gieger, et al., Metabolic profiling reveals distinct variations linked to nicotine consumption in humans—first results from the KORA study, PLoS One 3 (2008), e3863.
[55] S.V. Pande, A mitochondrial carnitine acylcarnitine translocase system, Proc. Natl. Acad. Sci. U. S. A. 72 (1975) 883–887.
[56] M. Perez-Carreras, P. Del Hoyo, M.A. Martin, J.C. Rubio, A. Martin, G. Castellano, et al., Defective hepatic mitochondrial respiratory chain in patients with nonalcoholic steatohepatitis, Hepatology 38 (2003) 999–1007.
[57] W. Roschinger, A.C. Muntau, M. Duran, L. Dorland, L. IJ, R.J. Wanders, et al., Carnitine–acylcarnitine translocase deficiency: metabolic consequences of an impaired mitochondrial carnitine cycle, Clin. Chim. Acta 298 (2000) 55–68.
[58] Y.A. Carpentier, L. Portois, A. Sener, W.J. Malaisse, Correlation between liver and plasma fatty acid profile of phospholipids and triglycerides in rats, Int. J. Mol. Med. 22 (2008) 255–262.
[59] L. Marai, A. Kuksis, Molecular species of lecithins from erythrocytes and plasma of man, J. Lipid Res. 10 (1969) 141–152.
[60] R. Wood, R.D. Harlow, Structural studies of neutral glycerides and phosphoglycerides of rat liver, Arch. Biochem. Biophys. 131 (1969) 495–501.
[61] H. Harizi, J.B. Corcuff, N. Gualde, Arachidonic-acid-derived eicosanoids: roles in biology and immunopathology, Trends Mol. Med. 14 (2008) 461–469.
[62] P. Dewing, T. Shi, S. Horvath, E. Vilain, Sexually dimorphic gene expression in mouse brain precedes gonadal differentiation, Brain Res. Mol. Brain Res. 118 (2003) 82–90.
[63] B. Jeffery, A.I. Choudhury, N. Horley, M. Bruce, S.R. Tomlinson, R.A. Roberts, et al., Peroxisome proliferator activated receptor alpha regulates a male-specific cytochrome P450 in mouse liver, Arch. Biochem. Biophys. 429 (2004) 231–236.
[64] C.J. Krebs, S. Khan, J.W. MacDonald, M. Sorenson, D.M. Robins, Regulator of sex-limitation KRAB zinc finger proteins modulate sex-dependent and -independent liver metabolism, Physiol. Genomics 38 (2009) 16–28.
[65] K. Jarukamjorn, T. Sakuma, N. Nemoto, Sexual dimorphic expression of mouse hepatic CYP2B: alterations during development or after hypophysectomy, Biochem. Pharmacol. 63 (2002) 2037–2041.
[66] T.L. Conforto, Y. Zhang, J. Sherman, D.J. Waxman, Impact of CUX2 on the female mouse liver transcriptome: activation of female-biased genes and repression of male-biased genes, Mol. Cell. Biol. 32 (2012) 4611–4627.
[67] J.A. Vizcaíno, E.W. Deutsch, R. Wang, A. Csordas, F. Reisinger, D. Ríos, et al., ProteomeXchange provides globally coordinated proteomics data submission and dissemination, Nat. Biotechnol. 32 (2014) 223–226.